Dalton Transactions



COMMUNICATION

View Article Online
View Journal | View Issue



Cite this: *Dalton Trans.*, 2024, **53**, 894

Received 11th December 2023, Accepted 18th December 2023 DOI: 10.1039/d3dt04141q

rsc.li/dalton



Yan Peng, (1) *a,b Jonas Braun, (1) a,c,d Michael Schulze, (1) e Hagen Kaemmerer, (1) a,d Yannik F. Schneider, (1) a,c Christopher E. Anson, (1) a Wolfgang Wernsdorfer (1) d,e and Annie K. Powell (1) *a,b,d

The 20-nuclearity compound $[Fe_8Dy_{12}(tea)_8(teaH)_{12}(NO_3)_{12}]$. 8MeCN (where $teaH_3$ = triethanolamine) was synthesised and characterised through single crystal X-ray diffraction and magnetic measurements. The shape of the magnetic hysteresis in the microSQUID measurements was rationalised using the MAGELLAN program.

Investigations on coordination clusters (CCs) based on either 3d or 4f ions have attracted great attention over the past decades because of their beautiful molecular architectures and interesting magnetic properties, such as single molecule magnet (SMM) behaviour, 1-3 the magnetocaloric effect 4-8 and spintronics.9 Particular attention has been paid to cyclic coordination clusters (CCCs), whose closed but infinite electronic structure could have applications in molecular electronics/spintronics and have, for example, been identified as qubits.10 Pioneering research has shown many examples of homometallic wheel-shaped clusters such as {Mo₁₅₄}, 11 $\{Mn_{84}\}$, 12 $\{Ni_{24}\}$, 13 $\{Dy_{21}\}^{14}$ and $\{Gd_{140}\}$. 15 However, heterometallic cyclic clusters containing cooperatively coupled 3d and 4f ions have rarely been reported. Most of the examples, including $\{M_4Ln_4\}$ $(M=Fe^{III}, Cr^{III}, Mn^{III})$, $^{16-19}$ $\{Fe_4Ln_2\}$, 20,21 $\{Fe_5Yb_3\}$, 21 $\{Fe_3Yb_2\}$, 21 $\{Fe_{16}Ln_4\}$, 22 $\{Fe_{10}Ln_{10}\}^{21,23,24}$ and ${\left\{Fe_{18}Dy_{6}\right\}}^{25,26}$ complexes, were reported by Powell and coworkers. Examples of other 3d-4f wheel motifs include

 ${\rm \{Mn_8Ln_8\}},^{27}$ ${\rm \{Cr_8Ln_8\}},^{28}$ ${\rm \{Cu_{36}Ln_{24}\}}^{29}$ and ${\rm \{Co_{16}Ln_{24}\}}^{30}$ complexes reported by other groups. It is noted that the common features in the synthesis of these 3d–4f cyclic structures are the use of amine polyalcohol ligands such as triethanolamine and N^{-n} butyldiethanolamine, and small bridging co-ligands, like acetate, benzoate and α -amino acids.

Cyclic systems containing paramagnetic ions, in particular Dy^{III}, have the possibility to show toroidal moments which lead to non-magnetic states. Such a toroidal moment can have a spin structure which is either a cyclic arrangement of the spin in the metal ion plane or a solenoidal arrangement, both of which lead to non-magnetic states. For coordination systems the first molecule to be identified showing such an arrangement was a Dy₃ triangle.^{31–33} Since then many more molecular systems have been identified, as recently summarised in Murray's book *Single Molecule Toroics*.³⁴

The compound we report here has the same overall nuclearity as the $Fe_{10}Ln_{10}$ clusters we previously described. These exhibited quantum properties such as proximity to the quantum critical point, exciton formation and intermolecular charge hopping.^{21,23} By slightly modifying the synthetic procedure we obtained an Fe_8Dy_{12} coordination cluster and report here the investigation of its magnetic properties.

The reaction of $Fe(NO_3)_3 \cdot 9H_2O$ and $Dy(NO_3)_3 \cdot 6H_2O$ with $teaH_3$ in MeOH and MeCN in the presence of Et_3N at ambient temperature yielded $[Fe_8Dy_{12}(Htea)_8(tea)_{12}(NO_3)_{12}] \cdot 8MeCN$ (1). Single-crystal X-ray diffraction studies reveal that compound (1) crystallises in the tetragonal space group $I4_1/acd$ (Fig. 1). The molecule is on a twofold axis in the crystal and thus the asymmetric unit is half the molecule (Fig. S1†).

Compound 1 is related to the previously reported $[Fe_{10}Ln_{10}(Me\text{-tea})_{10}(Me\text{-teaH})_{10}(NO_3)_{10}]$. The repeating units of both nanoscale compounds are extremely similar as both show Dy-Fe-Dy-Fe-Dy chains (Fig. 2), but rather than the Fe^{III} ion that follows, leading to alternating Fe-Dy in the $\{Fe_{10}Dy_{10}\}$ ring, these units are linked by an additional Dy^{III} ion in $\{Fe_8Dy_{12}\}$ (1). This also influences the topology of the cluster. While $\{Fe_{10}Dy_{10}\}$ can be described as a cyclic standing

^aInstitute of Inorganic Chemistry, Karlsruhe Institute of Technology (KIT), Kaiserstr. 12, 76131 Karlsruhe, Germany. E-mail: annie.powell@kit.edu

^bSchool of Chemistry and Chemical Engineering, Jiangxi University of Science and Technology, Ganzhou 341000, P.R. China

^cInstitute of Nanotechnology (INT), Karlsruhe Institute of Technology (KIT), Kaiserstr. 12. 76131 Karlsruhe. Germany

^dInstitute for Quantum Materials and Technologies (IQMT), Karlsruhe Institute of Technology (KIT), Kaiserstr. 12, 76131 Karlsruhe, Germany

^ePhysikalisches Institut, Karlsruhe Institute of Technology (KIT), Kaiserstr. 12, 76131 Karlsruhe, Germany

[†] Electronic supplementary information (ESI) available: Experimental and further magnetic data together with crystallographic data in CIF format. CCDC 2306455. For ESI and crystallographic data in CIF or other electronic format see DOI: https://doi.org/10.1039/d3dt04141g

Dalton Transactions Communication

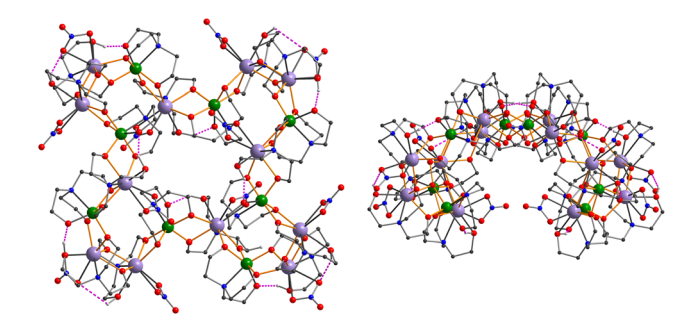


Fig. 1 Two views of the molecular structure of Fe₈Dy₁₂ (1).

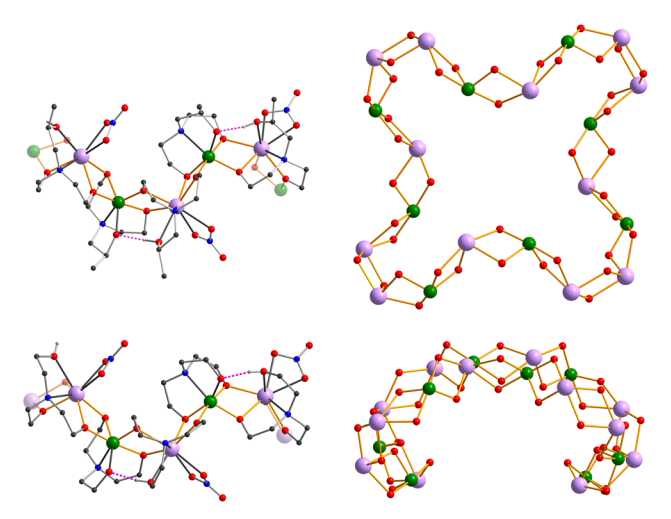


Fig. 2 Comparison of the repeating units of $Fe_{10}Dy_{10}$ (top, left) and Fe_8Dy_{12} (1) (bottom, left) with the difference in the continuation of the chain having paler coloured Fe/Dy ions as appropriate. Two views of the saddle-like core structure of 1 (right).

wave, the presence of additional Dy^{III} ions leads to the cluster folding into a saddle shape (Fig. 2). Within 1, the Fe^{III} ion is chelated by the nitrogen and three oxygen atoms of a fully deprotonated tea^{3-} ligand and the Dy^{III} ions by a doubly deprotonated $teaH^{2-}$ ligand with one alcohol arm remaining protonated. The two deprotonated alcohol arms of each ligand form μ -alkoxo bridges to adjacent metal centres in the ring.

The static magnetic susceptibilities of compound 1 were collected over the temperature range 1.8–300 K under an applied magnetic field of 0.1 T. Magnetisation data were collected at fields of 0–7 T at temperatures of 2, 3 and 5 K. The χT value of 1 is 204.7 cm³ K mol⁻¹ at 300 K, close to the expected value of 205.1 cm³ K mol⁻¹ for eight uncoupled Fe^{III} and twelve Dy^{III} ions (Fig. 2). Upon cooling, the χT value stays nearly constant before increasing sharply below 30 K reaching a maximum value of 246.9 cm³ K mol⁻¹ at 4.3 K. This is followed by an abrupt decrease at lower temperature to 200.6 cm³ K mol⁻¹ at 1.8 K. The increase of the χT value suggests ferromagnetic coupling between Fe^{III} and Dy^{III} ions, while the subsequent decrease is likely due to the presence of magnetic anisotropy and/or intermolecular weak antiferromagnetic interactions. The presence of dominant ferro-

magnetic intramolecular interactions is supported by the temperature dependence of the reciprocal susceptibility $(1/\chi)$ over the whole temperature range following the Curie–Weiss law $(\chi = C/(T - \theta))$ with a Weiss constant $\theta = +0.54$ K and Curie Constant C = 203 cm³ K mol⁻¹ (Fig. 3, top). The field-dependent magnetisation measurements for **1** (Fig. 3, bottom) increase sharply at low fields and reach $95.80\mu_{\rm B}$ at 7 T without reaching saturation, suggesting the presence of significant magnetic anisotropy.

To probe the magnetic anisotropy, ac susceptibility measurements were carried out under zero dc field for compound 1. Out-of-phase signals were detected below 5 K (Fig. S3†) indicative of the slow relaxation of the magnetisation behaviour characteristic of potential SMMs. Under a small external dc field, the magnetic slow relaxation was still too fast for maxima to be observed (Fig. S4†) within the parameters of our SQUID.

MicroSQUID measurements were performed at different temperatures and scan rates (Fig. 4 and S5†). In order to investigate the energy barrier and relaxation time, dc magnetisation decay measurements were performed under zero applied field in the sub-kelvin temperature range (Fig. S5†). The relaxation times were fitted using the following equation:

$$\tau^{-1} = AT + B + CT^{n} + {\tau_0}^{-1} \exp(-U_{\text{eff}}/k_{\text{B}}T)$$

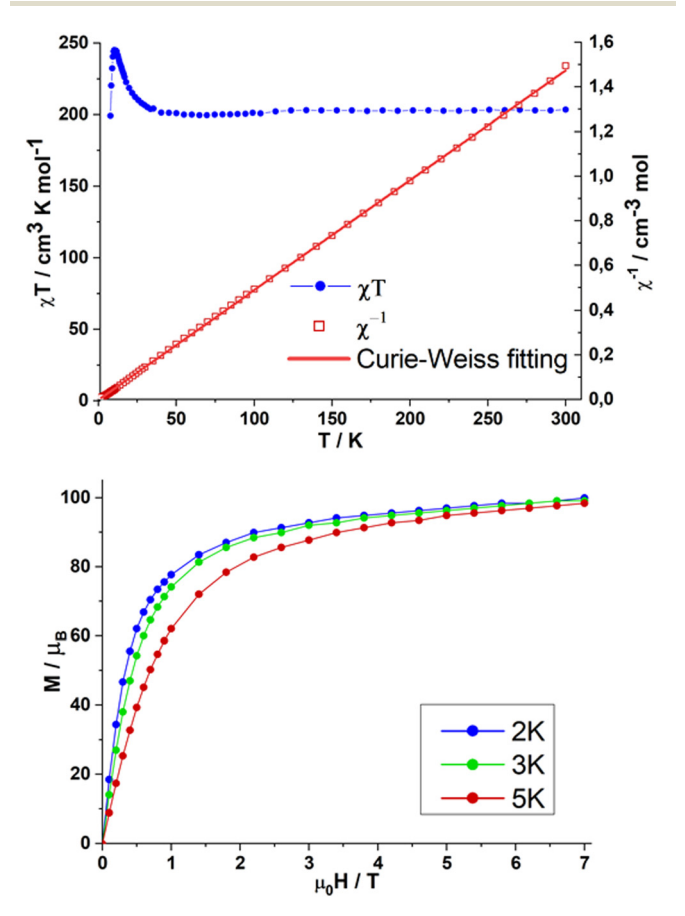
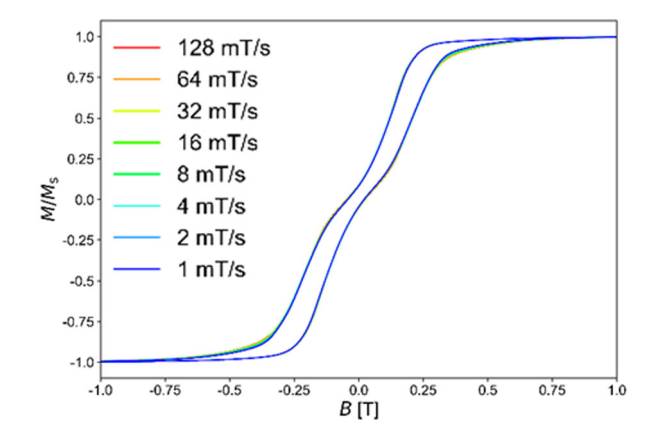


Fig. 3 Magnetic dc (top) and magnetisation data (bottom) for Fe_8Dy_{12} (1).

Communication **Dalton Transactions**



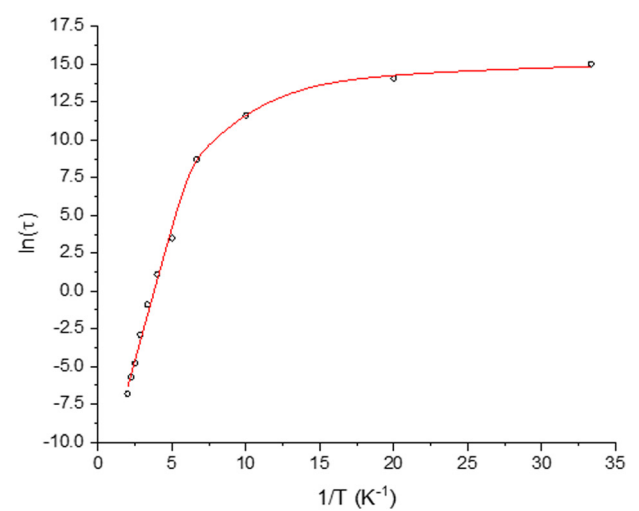


Fig. 4 MicroSQUID measurement of the sweep rate dependence of the magnetisation at T=30 mK (top). Plot of relaxation time (τ) against T^{-1} for complex (1) using dc magnetisation decay data (bottom). The red line is a fit of the relaxation data to the equation described above.

where A describes the direct process, B describes the zero field quantum tunnelling (ZFQTM), C is the Raman process with the Raman exponent n, τ_0 is the preexponential factor and $U_{\rm eff}$ is the energy barrier related to the Orbach process. The relaxation times of 1 could be fitted without the need for the parameter B, thus excluding the presence of ZFQTM which is also clear from the absence of a vertical increase at 0 T in the microSQUID hysteresis loops. The parameters for the best fit are $A = 1.18 \times 10^{-5} \text{ s}^{-1} \text{ K}^{-1}$, B = 0, $C = 90.4 \text{ s}^{-1} \text{ K}^{-n}$, n = 7.05, τ_0 = 1.49×10^{-6} s and the extracted energy barrier U_{eff} is 3.54 K.

In order to understand the hysteresis behaviour seen in the microSQUID measurement we performed the electrostatic field-based MAGELLAN35 analysis to locate the Ising easy-axes of the DyIII ions. Although this program was designed for purely Dy^{III} containing molecules, nevertheless we have found that coordination clusters containing Fe^{III} and Dy^{III} can be safely analysed. Furthermore, a cluster of this size cannot be calculated using ab initio methods; therefore MAGELLAN provides the only opportunity to help rationalise the magnetic behaviour. Whereas in the Fe₁₀Dy₁₀ cluster the axes are

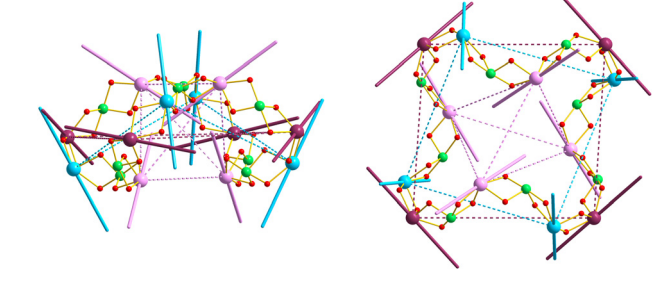


Fig. 5 Two views of the core structure of compound (1) showing the three sets of MAGELLAN axes. The pink set represents the spin-ice-like structure, the burgundy set represents the toroidal "square" and the cyan set represents the boat-like shape.

arranged in a regular arrangement (see Fig. S6†), the saddleshape of 1 leads to an apparent jumble of directions (see Fig. 5). However, a closer analysis reveals that in fact the twelve Dy^{III} ions can be divided into three sets of four ions (see Fig. 5). The innermost set of four corresponds to a slightly distorted tetrahedron with its MAGELLAN axes oriented in a spinice-like arrangement (pink in Fig. 5).36,37 The middle set of axes form what can be described as a toroidal arrangement around a slightly distorted square as seen for Dy. 38 The "square" is neither completely planar nor completely square, but with angles of 86.3° and 93.7° as well as distances of 12.8 Å and 13.3 Å, and the deviation from planarity for each of the Dy^{III} ions of 0.32 Å is not far off (burgundy in Fig. 5). The outer set is arranged in a boat-like shape. Two of the axes are parallel and essentially perpendicular to the plane of the "square" of the middle layer. The other two are at an angle of 30.1° to the perpendicular ones (cyan in Fig. 5).

These arrangements may lead to the following characteristics of the microSQUID hysteresis curve. The easiest part to assess is the toroidal nature of the middle set which leads to a narrowing and a change in gradient near 0 T. The alignment of the outer set is likely responsible for the sharp increase in magnetisation at fields higher than 0.1 T. The inner spin-icelike set remains a "dark horse" in the sense that its contribution to the magnetic hysteresis behaviour is impossible to judge but it might possibly be non-magnetic.

In conclusion, disrupting the alternating pattern of the ions in the Fe₁₀Ln₁₀ ring system through slightly altered reaction conditions leads to a folding of the ring into a saddle shape. This in turn alters the orientations of the MAGELLAN axes. These axes help rationalise the magnetic hysteresis observed in the microSQUID measurements.

Author contributions

Y.P. and Y.F.S.: synthesis and characterisation; J.B., H.K., C.E. A. and A.K.P.: paper conceptualisation and writing; C.E.A.: crystallography; M.S. and W.W.: microSQUID measurement and interpretation; and A.K.P.: supervision and funding acquisition.

Dalton Transactions

Conflicts of interest

There are no conflicts to declare.

Acknowledgements

We acknowledge funding through DFG CRC 1573 "4f For Future" and the POF MSE Helmholtz Foundation, and J. B. and Y. F. S. acknowledge support from the Landesgraduiertenförderung Baden-Württemberg.

References

- 1 R. Sessoli, D. Gatteschi, A. Caneschi and M. A. Novak, *Nature*, 1993, **365**, 141–143.
- 2 R. Sessoli, H.-L. Tsai, A. R. Schake, S. Wang, J. B. Vincent, K. Folting, D. Gatteschi, G. Christou and D. N. Hendrickson, J. Am. Chem. Soc., 1993, 115, 1804–1816.
- 3 D. Gatteschi and R. Sessoli, *Angew. Chem., Int. Ed.*, 2003, 42, 268–297.
- 4 M. Evangelisti, F. Luis, L. J. de Jongh and M. Affronte, *J. Mater. Chem.*, 2006, **16**, 2534–2549.
- J. W. Sharples, Y. Z. Zheng, F. Tuna, E. J. McInnes and D. Collison, *Chem. Commun.*, 2011, 47, 7650–7652.
- 6 J. W. Sharples, D. Collison, E. J. L. McInnes, J. Schnack, E. Palacios and M. Evangelisti, *Nat. Commun.*, 2014, 5, 5321–5326.
- 7 Y. Z. Zheng, G. J. Zhou, Z. Zheng and R. E. Winpenny, Chem. Soc. Rev., 2014, 43, 1462–1475.
- 8 T. G. Tziotzi, D. Gracia, S. J. Dalgarno, J. Schnack, M. Evangelisti, E. K. Brechin and C. J. Milios, *J. Am. Chem. Soc.*, 2023, 145, 7743–7747.
- 9 L. Bogani and W. Wernsdorfer, *Nat. Mater.*, 2008, 7, 179– 186.
- 10 G. A. Timco, S. Carretta, F. Troiani, F. Tuna, R. J. Pritchard, C. A. Muryn, E. J. McInnes, A. Ghirri, A. Candini, P. Santini, G. Amoretti, M. Affronte and R. E. Winpenny, *Nat. Nanotechnol.*, 2009, 4, 173–178.
- 11 T. Liu, E. Diemann, H. Li, A. W. M. Dress and A. Müller, *Nature*, 2003, **426**, 59–62.
- 12 A. J. Tasiopoulos, A. Vinslava, W. Wernsdorfer, K. A. Abboud and G. Christou, *Angew. Chem.*, *Int. Ed.*, 2004, 43, 2117–2121.
- 13 A. L. Dearden, S. Parsons and R. E. P. Winpenny, *Angew. Chem., Int. Ed.*, 2001, **40**, 151–154.
- 14 S. Biswas, S. Das, J. Acharya, V. Kumar, J. van Leusen, P. Kogerler, J. M. Herrera, E. Colacio and V. Chandrasekhar, *Chem. - Eur. J.*, 2017, 23, 5154–5170.
- 15 X.-Y. Zheng, Y.-H. Jiang, G.-L. Zhuang, D.-P. Liu, H.-G. Liao, X.-J. Kong, L.-S. Long and L.-S. Zheng, *J. Am. Chem. Soc.*, 2017, 139, 18178–18181.
- 16 M. Li, A. M. Ako, Y. Lan, W. Wernsdorfer, G. Buth, C. E. Anson, A. K. Powell, Z. Wang and S. Gao, *Dalton Trans.*, 2010, 39, 3375–3377.

- 17 M. Li, Y. Lan, A. M. Ako, W. Wernsdorfer, C. E. Anson, G. Buth, A. K. Powell, Z. Wang and S. Gao, *Inorg. Chem.*, 2010, 49, 11587–11594.
- 18 J. Rinck, G. Novitchi, W. Van den Heuvel, L. Ungur, Y. Lan, W. Wernsdorfer, C. E. Anson, L. F. Chibotaru and A. K. Powell, *Angew. Chem.*, *Int. Ed.*, 2010, 49, 7583–7587.
- 19 D. Schray, G. Abbas, Y. Lan, V. Mereacre, A. Sundt, J. Dreiser, O. Waldmann, G. E. Kostakis, C. E. Anson and A. K. Powell, Angew. Chem., Int. Ed., 2010, 49, 5185–5188.
- 20 S. Schmidt, D. Prodius, G. Novitchi, V. Mereacre, G. E. Kostakis and A. K. Powell, *Chem. Commun.*, 2012, 48, 9825–9827.
- 21 A. Baniodeh, C. E. Anson and A. K. Powell, *Chem. Sci.*, 2013, 4, 4354–4361.
- 22 A. Baniodeh, I. J. Hewitt, V. Mereacre, Y. Lan, G. Novitchi, C. E. Anson and A. K. Powell, *Dalton Trans.*, 2011, 40, 4080– 4086.
- 23 A. Baniodeh, Y. Liang, C. E. Anson, N. Magnani, A. K. Powell, A.-N. Unterreiner, S. Seyfferle, M. Slota, M. Dressel, L. Bogani and K. Goß, *Adv. Funct. Mater.*, 2014, 24, 6280–6290.
- 24 J. R. Machado, A. Baniodeh, A. K. Powell, B. Luy, S. Kramer and G. Guthausen, *ChemPhysChem*, 2014, 15, 3608–3613.
- 25 O. Botezat, J. van Leusen, V. C. Kravtsov, P. Kögerler and S. G. Baca, *Inorg. Chem.*, 2017, **56**, 1814–1822.
- 26 H. Kaemmerer, A. Baniodeh, Y. Peng, E. Moreno-Pineda, M. Schulze, C. E. Anson, W. Wernsdorfer, J. Schnack and A. K. Powell, J. Am. Chem. Soc., 2020, 142, 14838–14842.
- 27 K. R. Vignesh, S. K. Langley, B. Moubaraki, K. S. Murray and G. Rajaraman, *Chem. Eur. J.*, 2015, **21**, 16364–16369.
- 28 L. Qin, J. Singleton, W. P. Chen, H. Nojiri, L. Engelhardt, R. E. P. Winpenny and Y. Z. Zheng, *Angew. Chem., Int. Ed.*, 2017, 56, 16571–16574.
- 29 J. D. Leng, J. L. Liu and M. L. Tong, Chem. Commun., 2012, 48, 5286–5288.
- 30 Z.-M. Zhang, L.-Y. Pan, W.-Q. Lin, J.-D. Leng, F.-S. Guo, Y.-C. Chen, J.-L. Liu and M.-L. Tong, *Chem. Commun.*, 2013, 49, 8081–8083.
- 31 J. Tang, I. Hewitt, N. T. Madhu, G. Chastanet, W. Wernsdorfer, C. E. Anson, C. Benelli, R. Sessoli and A. K. Powell, *Angew. Chem.*, 2006, **118**, 1761.
- 32 L. F. Chibotaru, L. Ungur and A. Soncini, *Angew. Chem.*, 2008, **120**, 4194–4197.
- 33 J. Luzon, K. Bernot, I. J. Hewitt, C. E. Anson, A. K. Powell and R. Sessoli, *Phys. Rev. Lett.*, 2008, **100**, 247205.
- 34 K. Murray, *Single Molecule Toroics*, Springer Nature Switzerland AG, Cham, 2022.
- 35 N. F. Chilton, D. Collison, E. J. McInnes, R. E. Winpenny and A. Soncini, *Nat. Commun.*, 2013, 4, 2551.
- 36 C. Kachi-Terajima, T. Eiba, R. Ishii, H. Miyasaka, Y. Kodama and T. Saito, *Angew. Chem., Int. Ed.*, 2020, 59, 22048–22053.
- 37 C. Castelnovo, R. Moessner and S. L. Sondhi, *Annu. Rev. Condens. Matter Phys.*, 2012, 3, 35–55.
- 38 G. Abbas, Y. Lan, G. E. Kostakis, W. Wernsdorfer, C. E. Anson and A. K. Powell, *Inorg. Chem.*, 2010, **49**, 8067–8072.